Fractional vortices and composite domain walls in flat nanomagnets

Oleg Tchernyshyov and Gia-Wei Chern

Department of Physics and Astronomy, The Johns Hopkins University, Baltimore, Maryland, 21218, USA (Dated: 11 September 2005)

We provide a simple explanation of complex magnetic patterns observed in ferromagnetic nanostructures. To this end we identify elementary topological defects in the field of magnetization: ordinary vortices in the bulk and vortices with half-integer winding numbers confined to the edge. Domain walls found in experiments and numerical simulations in strips and rings are composite objects containing two or more of the elementary defects.

Topological defects [1, 2] greatly influence the properties of materials by catalyzing or inhibiting the switching between differently ordered states. In ferromagnetic nanoparticles of various shapes (e.g. strips [3] and rings [4]), the switching process involves creation, propagation, and annihilation of domain walls with complex internal structure [5]. Here we show that these domain walls are composite objects made of two or more elementary defects: vortices with integer winding numbers $(n = \pm 1)$ and edge defects with fractional winding numbers $(n = \pm 1/2)$. The simplest domain walls are composed of two edge defects with opposite winding numbers. Creation and annihilation of the defects is constrained by conservation of a topological charge. This framework provides a basic understanding of the complex switching processes observed in ferromagnetic nanoparticles.

In ferromagnets the competition between exchange and magnetic dipolar energies creates nonuniform patterns of magnetization in the ground state. Whereas the exchange energy favors a state with uniform magnetization, magnetic dipolar interactions align the vector of magnetization with the surface. In a large magnet a compromise is reached by the formation of uniformly magnetized domains separated by domain walls. In a nanomagnet magnetization varies continuously forming intricate vet highly reproducible textures, which include domain walls and vortices [5, 6, 7]. Numerical simulations [8, 9] reveal a rich internal structure and complex dynamics of these objects. For example, collisions of two domain walls can have drastically different outcomes: complete annihilation or formation of other stable textures [7]. These puzzling phenomena call for a theoretical explanation.

An elementary picture of topological defects in nanomagnets with a planar geometry is presented in this Letter. It is suggested that the *elementary* defects are vortices with integer winding numbers and edge defects with half-integer winding numbers. All of the intricate textures, including the domain walls, are *composite* objects made of two or more elementary defects.

For simplicity, we consider a ferromagnet without intrinsic anisotropy, which is a good approximation for permalloy. The magnetic energy consists of two parts: the exchange contribution $A \int |\nabla \hat{\mathbf{m}}| \, d^3 r$, where $\hat{\mathbf{m}} = \mathbf{M}/|\mathbf{M}|$ is the unit vector pointing in the direc-

tion of magnetization \mathbf{M} , and the magnetostatic energy $(\mu_0/2)\int |\mathbf{H}|^2 d^3r$. The magnetic field \mathbf{H} is related to the magnetization through Maxwell's equations, $\nabla \times \mathbf{H} = 0$ and $\nabla \cdot (\mathbf{H} + \mathbf{M}) = 0$. Apart from a few special cases (e.g. an ellipsoidal particle), finding configurations $\hat{\mathbf{m}}(\mathbf{r})$ of lowest energy is a difficult computational problem.

Analytical treatment is nonetheless possible in a thinfilm limit [10, 11] defined for a strip of width w and thickness t as

$$t \ll w \ll \lambda^2 / t \ll w \log(w/t), \tag{1}$$

where $\lambda = \sqrt{A/\mu_0 M^2}$ is a magnetic length scale (5 nm in permalloy). Taking this limit yields three simplifications: (a) magnetization lies in the plane of the film, $\hat{\mathbf{m}} = (\cos \theta, \sin \theta, 0)$; (b) it depends on the in-plane coordinates x and y, but not on z; (c) the magnetic energy becomes a local functional of magnetization [10, 11]:

$$E[\hat{\mathbf{m}}(\mathbf{r})]/At = \int_{\Omega} |\nabla \hat{\mathbf{m}}|^2 d^2r - (1/\Lambda) \int_{\partial \Omega} (\hat{\mathbf{m}} \cdot \hat{\boldsymbol{\tau}})^2 dr.$$
 (2)

The quantity E/At is a dimensionless energy, Ω is the two-dimensional region of the film, $\partial\Omega$ is its line boundary, $\hat{\tau} = (\cos\theta_{\tau}, \sin\theta_{\tau}, 0)$ is the unit vector parallel to the boundary, and $\Lambda = 4\pi\lambda^2/t\log(w/t)$ is the effective magnetic length in the thin-film geometry. The first—exchange—term in Eq. (2) is the familiar XY model [1] with the ground states obeying the Laplace equation $\nabla^2\theta = 0$ in the bulk. The second term expresses the magnetostatic energy due to magnetic charges at the film edge and sets the boundary conditions.

Things are particularly simple in the limit $\Lambda/w \to 0$, when magnetization at the edge is forced to be parallel to the boundary, $\hat{\mathbf{m}} = \pm \hat{\tau}$. Solutions in this limit can be constructed by exploiting the analogy between the XY model and electrostatics in two dimensions [1], whereby the angle gradients are associated with components of the electric field, $(E_x, E_y) = (\partial_y \theta, -\partial_x \theta)$. Topological defects—vortices with winding numbers $n = \pm 1$ —become positive and negative point charges of unit strength. In the presence of an edge, solutions are obtained by the method of images. For instance, a single vortex (winding number $n = \pm 1$) located at (X, Y) in the infinite semiplane y > 0 is

$$\theta(x,y) = \pm \arctan\left(\frac{y-Y}{x-X}\right) \pm \arctan\left(\frac{y+Y}{x-X}\right).$$
 (3)

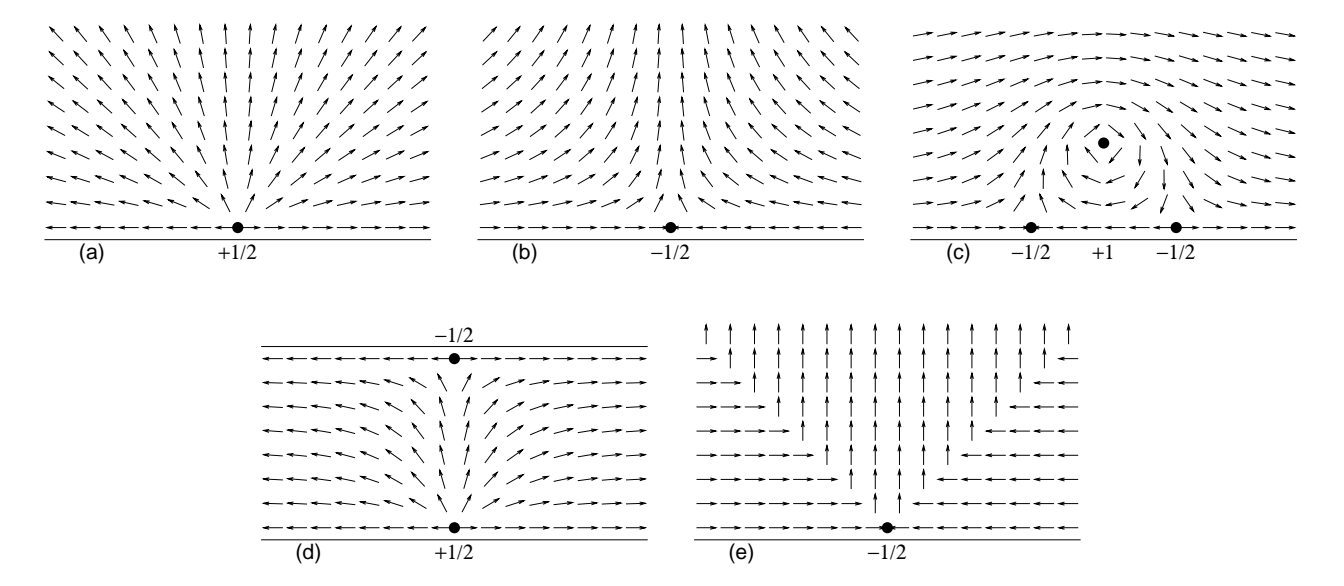


FIG. 1: (a) and (b) Edge defects with winding numbers $n=+\frac{1}{2}$ and $-\frac{1}{2}$. (c) A vortex (n=+1) offsets the influence of two $-\frac{1}{2}$ edge defects. (d) A domain wall composed of two edge defects $\pm\frac{1}{2}$. (e) The $-\frac{1}{2}$ defect in the limit where magnetostatic energy dominates.

The image "charge" at (X, -Y) has the same sign as the original. Therefore, a vortex is repelled by the boundary.

Another class of solutions [Fig. 1(a) and (b)] has a singularity at the edge [10]:

$$\theta(x,y) = \pm \arctan\left(\frac{y}{x-X}\right).$$
 (4)

In the spirit of Eq. (3), this solution can be viewed as a halfvortex whose winding number $\pm \frac{1}{2}$ is doubled by the reflection in the edge. Confinement to the edge occurs because vortices with noninteger winding numbers cannot exist in the bulk. An attempt to peel a halfvortex away from the edge will make $\theta(x, y)$ a multivalued function:

$$\theta(x,y) = \pm \frac{1}{2} \arctan\left(\frac{y-Y}{x-X}\right) \pm \frac{1}{2} \arctan\left(\frac{y+Y}{x-X}\right).$$
 (5)

The multivaluedness means that the magnetization will be discontinuous across a line defect extending from the core of the halfvortex to the film boundary and thus providing a potential $V \propto Y$ confining the halfvortex to the edge.

The assignment of fractional winding numbers to edge defects can be justified in a more direct way: a superposition of two edge defects and one vortex (n=+1) has zero total defect strength [Fig. 1(c)]. Hence $n=-\frac{1}{2}$ for each of the edge defects. A model-independent, purely geometrical justification will be given below.

In a strip |y| < w/2, a domain wall interpolating between the $\theta = 0$ and π ground states can be constructed out of two edge defects with opposite winding numbers

 $\pm \frac{1}{2}$ and $\mp \frac{1}{2}$ [Fig. 1(d)]:

$$\tan \theta(x, y) = \pm \frac{\cos (\pi y/w)}{\sinh (\pi (x - X)/w)}.$$
 (6)

It is clear from the electrostatic analogy that the two defects experience an attractive "Coulomb" force (not strong enough to overcome the edge confinement). This force holds the composite domain wall together. Because the XY model itself contains no length scale, the extent of the domain wall along the strip is set by the width of the strip w. This is precisely the kind of a domain wall observed in numerical simulations [9].

The above solutions can be easily adopted to the cases when the ratio Λ/w is small but finite. The singular cores of the halfvortices reside outside the film, the distance Λ away from the edge [10].

The topological defects identified above survive well outside the range of applicability of the model (2). Fig. 2 shows simulated dynamics in a permalloy disk of the diameter w=400 nm and thickness t=20 nm. (We used the numerical package OOMMF [12].) Inequality (1) fails badly, yet the bulk and edge defects are easily recognisable and the winding numbers are clearly conserved.

In wider and thicker strips $(wt \gtrsim \lambda^2)$, the magnetostatic energy breaks the symmetry between the defects with positive and negative winding numbers inherent to the XY model. In particular, the $+\frac{1}{2}$ edge defects have a higher magnetostatic energy than their $-\frac{1}{2}$ counterparts. Evidence for this can be seen in numerical simulations [9] showing a more substantial broadening of the cores in $n = +\frac{1}{2}$ defects.

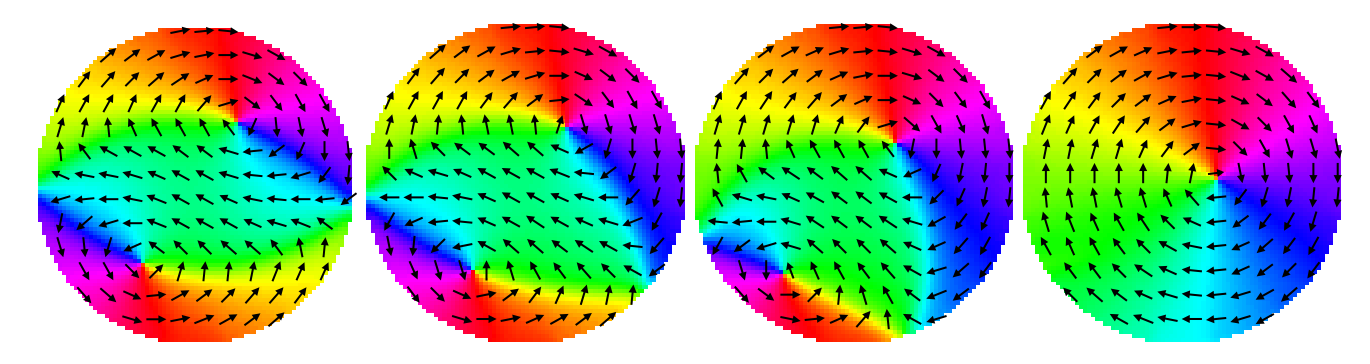


FIG. 2: Numerical simulation of magnetization dynamics in a permalloy disk. Color encodes the direction of the field $\hat{\mathbf{m}}$ (also shown by arrows). Convergence of different colors at a point signals the presence of a topological defect. In the first three panels the disk contains two +1 vortices and two $-\frac{1}{2}$ edge defects. After the edge defects and a vortex mutually annihilate (last panel), a single vortex remains.

In the magnetostatic regime $wt\gg\lambda^2$, the defects can again be constructed explicitly [13]. The magnetostatic energy is minimized if the density of magnetic charges vanishes in the bulk, $\nabla\cdot\hat{\mathbf{m}}=0$, and on the surface, $\hat{\mathbf{m}}=\pm\hat{\boldsymbol{\tau}}$. It can be checked that the +1 vortex in the bulk retains its shape [Fig. 1(c)]. The $-\frac{1}{2}$ edge defect looks like two domain walls emanating from a point at the edge in orthogonal directions [Fig. 1(e)]. The -1 vortex is a similar intersection of four domain walls. The V-shaped $-\frac{1}{2}$ edge defects can be seen in numerical simulations [9]. Domain walls in this limit are made of two $-\frac{1}{2}$ defects and a +1 vortex between them [13]. This type of the domain wall is favored when $wt\gtrsim C\lambda^2$, where $C\approx 130$ is a rather large numerical parameter [9] weakly dependent on the thickness t.

Although different in shape, the $-\frac{1}{2}$ edge defects in the exchange [Fig. 1(b)] and magnetostatic [Fig. 1(e)] limits

have identical topological properties. Generally, as long as magnetization tends to align itself with the boundary, the edge defects are stable. They are manifested as kinks in magnetization $\hat{\mathbf{m}}$: the latter rotates along the edge between the local tangential directions $+\hat{\boldsymbol{\tau}}$ and $-\hat{\boldsymbol{\tau}}$. The winding number of a kink is defined as the line integral along the boundary:

$$n = -\frac{1}{2\pi} \int_{\partial\Omega} \mathbf{\nabla} (\theta - \theta_{\tau}) \cdot d\mathbf{r} = \pm \frac{1}{2}$$
 (7)

for a single edge defect. Because the boundary $\partial\Omega$ is a closed line, it always contains an even number of kinks. The sum of the winding numbers of edge defects is thus an integer related to the topological charge of bulk defects. In a simply connected (no holes) region Ω ,

$$\sum_{i}^{\text{edge}} n_{i} = 1 - \frac{1}{2\pi} \oint_{\partial \Omega} \nabla \theta \cdot d\mathbf{r} = 1 - \frac{1}{2\pi} \int_{\Omega} (\partial_{x} \partial_{y} \theta - \partial_{y} \partial_{x} \theta) d^{2} r = 1 - \sum_{i}^{\text{bulk}} n_{i}, \tag{8}$$

with integer n_i for bulk defects. In a film with g holes,

$$\sum_{i} n_i = 1 - g. \tag{9}$$

The winding numbers are ± 1 for bulk defects and $\pm \frac{1}{2}$ for edge defects. The half-integer value of the topological charge is directly related to the presence of a kink in magnetization at the edge [14, 15, 16]. The halfvortices are analogs of the boojums thought to exist at an interface between the A and B phases of superfluid ³He [17, 18].

Conservation of topological charge (9) has important implications for the dynamics of magnetization in nanomagnets. For example, in rings of certain sizes the ground state contains no topological defects and has zero magnetic dipole moment [Fig. 3(a)]. The ring can be magnetized by applying a strong in-plane magnetic field. Switching off the field leaves the ring in a metastable state with remnant magnetization containing two composite domain walls [Fig. 3(b)]. By applying the magnetic field in the opposite direction, the walls can be set in motion on a collision course and may annihilate, leaving the magnet in a ground state [5]. However, direct annihilation of the two domain walls is impossible: both walls have the $-\frac{1}{2}$ defects at the inner edge of the ring and two such defects cannot annihilate on their own. Ac-

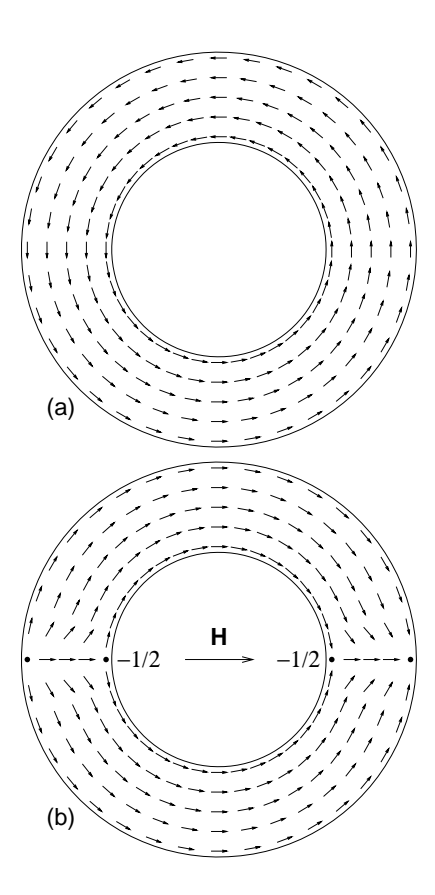


FIG. 3: Stable and metastable states of a magnetic nanoring in the thin-film limit. (a) One of the two ground states without topological defects. (b) State with a remnant magnetization contains two composite domain walls with $+\frac{1}{2}$ defects at the outer edge and $-\frac{1}{2}$ defects at the inner edge.

cordingly, in thin and narrow rings the two domain walls do not annihilate but instead form a "360° domain wall" [7]. In thicker and wider rings, the annihilation does occur and the ring returns to a ground state. To facilitate the annihilation, the edge defects in one of the domain walls must trade places. Because the edge defects themselves cannot move into the bulk, they alter the signs by exchanging a vortex. The $+\frac{1}{2}$ defect emits a +1 vortex into the bulk and converts into a $-\frac{1}{2}$ defect [19]. The emitted vortex travels to the inner edge where it fuses with the $-\frac{1}{2}$ defect into a $+\frac{1}{2}$ defect. Now the defects at both edges can annihilate directly. In thin and narrow rings this does not happen because vortex emission is forbidden energetically [9]. Transient states with vortices in the bulk of the ring have been observed in simulations [5]. However, their role in catalysing the annihilation of domain walls has not been appreciated.

We have uncovered a simple structure underlying intricate magnetic patterns in soft nanomagnets in a planar geometry. The patterns are formed by a few highly stable topological defects: ordinary vortices in the bulk and halfvortices confined to the edge. The importance of edge defects in nanomagnets has been overlooked. Here we have demonstrated that the "transverse" domain walls found in thin and narrow strips [9] are made of two such edge defects wiht opposite winding numbers. We will describe elsewhere [13] a simple model of the "vortex" domain walls [9] made of two $-\frac{1}{2}$ edge defects and a +1 vortex. It appears that the general approach taken in this paper may provide a basic model of complex magnetization dynamics in nanomagnets by reducing it to the creation, propagation, and annihilation of a few topological defects.

Acknowledgments. We thank C.-L. Chien, P. Fendley, R. L. Leheny, I. Tchernyshyov, and F. Q. Zhu for helpful discussions. The work was supported in part by the NSF Grant No. DMR05-20491.

- P. M. Chaikin and T. C. Lubensky, Principles of Condensed Matter Physics (Cambridge University Press, Cambridge, 2000).
- [2] N. D. Mermin, Rev. Mod. Phys. 51, 591 (1979).
- [3] D. Atkinson et al., Nature Mat. 2, 85 (2003).
- [4] J.-G. Zhu, Y. Zheng, and G. A. Prinz, J. Appl. Phys. 87, 6668 (2000).
- [5] M. Kläui, et al., J. Phys.: Condens. Matter 15, R985 (2003).
- [6] T. Shinjo, et al., Science 289, 930 (2000).
- [7] F. J. Castaño, et al., Phys. Rev. B 67, 184425 (2003).
- [8] J. Gadbois and J.-G. Zhu, IEEE Trans. Magn. **31**, 3802 (1995).
- [9] R. D. McMichael and M. J. Donahue, IEEE Trans. Magn. 33, 4167 (1997).
- [10] M. Kurzke, Calc. Var. PDE (in press).
- [11] R. V. Kohn and V. V. Slastikov, Proc. Roy. Soc. (London) Ser. A 461, 143 (2004).
- [12] M. J. Donahue and D. G. Porter, OOMMF User's Guide, Version 1.0, in *Interagency Report NISTIR 6376* (NIST, Gaithersburg, 1999). http://math.nist.gov/oommf/
- [13] G.-W. Chern, H. Youk, and O. Tchernyshyov, cond-mat/0508740; H. Youk, G.-W. Chern, K. Merit, B. Oppenheimer, and O. Tchernyshyov, cond-mat/0508741.
- [14] R. Jackiw and C. Rebbi, Phys. Rev. D 13, 3398 (1976).
- [15] J. Goldstone and F. Wilczek, Phys. Rev. Lett. 47, 986 (1981).
- [16] G. E. Volovik, J. Low. Temp. Phys. 121, 357 (2000).
- [17] T. Sh. Misirpashaev, Sov. Phys. JETP 72, 973(1991) [Zh. Eksp. Teor. Fiz. 99, 1741 (1991)].
- [18] G. E. Volovik, The Universe in a Helium Droplet (Clarendon Press, Oxford, 2003).
- [19] The same process also appears to take place in elliptical films. See P. Vavassori et al., Phys. Rev. B 69, 214404 (2004).